SPECIAL METABOLISM SECTION

Whole-Body Vibration Mimics the Metabolic Effects of Exercise in Male Leptin Receptor–Deficient Mice

Meghan E. McGee-Lawrence,[1] Karl H. Wenger,[2] Sudipta Misra,[3] Catherine L. Davis,[4,5] Norman K. Pollock,[4,5] Mohammed Elsalanty,[6] Kehong Ding,[7] Carlos M. Isales,[7] Mark W. Hamrick,[1] Marlena Wosiski-Kuhn,[5] Phonepasong Arounleut,[1] Mark P. Mattson,[8] Roy G. Cutler,[8] Jack C. Yu,[9] and Alexis M. Stranahan[7]

[1]Department of Cellular Biology and Anatomy, Medical College of Georgia, Augusta University, Augusta, Georgia 30912; [2]Department of Orthopedic Surgery, Medical College of Georgia, Augusta University, Augusta, Georgia 30912; [3]Department of Pediatrics, Gastroenterology Division, Medical College of Georgia, Augusta University, Augusta, Georgia 30912; [4]Georgia Prevention Institute, Medical College of Georgia, Augusta University, Augusta, Georgia 30912; [5]Physiology Department, Medical College of Georgia, Augusta University, Augusta, Georgia 30912; [6]Department of Oral Biology, Medical College of Georgia, Augusta University, Augusta, Georgia 30912; [7]Department of Neuroscience and Regenerative Medicine, Medical College of Georgia, Augusta University, Augusta, Georgia 30912; [8]Laboratory of Neurosciences, National Institute on Aging Intramural Research Program, Baltimore, Maryland 21224; and [9]Department of Surgery, Plastic Surgery Division, Medical College of Georgia, Augusta University, Augusta, Georgia 30912

Whole-body vibration (WBV) has gained attention as a potential exercise mimetic, but direct comparisons with the metabolic effects of exercise are scarce. To determine whether WBV recapitulates the metabolic and osteogenic effects of physical activity, we exposed male wild-type (WT) and leptin receptor–deficient (db/db) mice to daily treadmill exercise (TE) or WBV for 3 months. Body weights were analyzed and compared with WT and db/db mice that remained sedentary. Glucose and insulin tolerance testing revealed comparable attenuation of hyperglycemia and insulin resistance in db/db mice following TE or WBV. Both interventions reduced body weight in db/db mice and normalized muscle fiber diameter. TE or WBV also attenuated adipocyte hypertrophy in visceral adipose tissue and reduced hepatic lipid content in db/db mice. Although the effects of leptin receptor deficiency on cortical bone structure were not eliminated by either intervention, exercise and WBV increased circulating levels of osteocalcin in db/db mice. In the context of increased serum osteocalcin, the modest effects of TE and WBV on bone geometry, mineralization, and biomechanics may reflect subtle increases in osteoblast activity in multiple areas of the skeleton. Taken together, these observations indicate that WBV recapitulates the effects of exercise on metabolism in type 2 diabetes. (*Endocrinology* 158: 1160–1171, 2017)

Disruption of bone formation and turnover has been reported in a range of metabolic disorders, including obesity and type 2 diabetes. Although a significant body of literature suggests that obesity reduces risk of osteopenia and osteoporosis (1, 2), there are also numerous recent reports that obesity and its comorbidities reduce bone formation (3–6). Obesity is accompanied by ectopic lipid deposition in multiple tissues, including the skeleton, where infiltration of adipocytes into the bone marrow niche may negatively impact bone formation (7, 8). Bone marrow stem cells express receptors for multiple adipokines, including the adipose-derived hormone leptin

Abbreviations: ALT, alanine transaminase; ANOVA, analysis of variance; AST, aspartate aminotransferase; AUC, area under the curve; BMD, bone mineral density; EDL, extensor digitorum longus; ELISA, enzyme-linked immunosorbent assay; GGT, gamma glutamyl-transferase; H&E, hematoxylin and eosin; IP, intraperitoneal; IPGTT, intraperitoneal glucose tolerance testing; LDL, low-density lipoprotein; NEFA, nonesterified fatty acid; SED, sedentary; TE, treadmill exercise; vWAT, visceral white adipose tissue; WBV, whole-body vibration; WT, wild-type.

(9, 10). Data from leptin-deficient rodent models have revealed regionally specific effects on the skeleton, with reports of cortical bone atrophy in weight-bearing long bones like the femur and tibia (11–16). Leptin-deficient (ob/ob) mice also exhibit lower femoral cortical bone mineral density (BMD) and strength compared with wild-type (WT) littermates (13). Bone loss in models of leptin or leptin receptor deficiency has been linked with lower osteoblast activity (9, 14), suggesting that cellular leptin resistance in obesity might reduce bone formation.

Participation in regular physical activity protects against bone loss (12, 17), and increasing evidence suggests that whole-body vibration (WBV) elicits similar effects in certain patient populations (18–20). Bone is a mechanically responsive tissue (21, 22), and musculo-skeletal loading with WBV or exercise promotes bone formation in animal models (12, 21–26). Bone formation is accompanied by increased levels of osteocalcin, a hormone produced primarily by osteoblasts during matrix synthesis (7, 27, 28). Circulating osteocalcin also enhances insulin secretion by pancreatic β cells and increases levels of the insulin-sensitizing hormone adiponectin (29, 30). Circulating osteocalcin levels are reduced in humans and in rodent models of obesity and insulin resistance (16, 20, 31–34), and this effect is particularly prominent in models with coincident obesity and bone loss, such as Zucker rats (12) and leptin receptor–deficient (db/db) mice (16). However, no studies have directly compared the metabolic and skeletal consequences of WBV in parallel with physical exercise.

Given that exercise and WBV place biomechanical load on the skeleton, we hypothesized that both interventions would promote bone formation, and that osteogenic responses would be associated with improvements in glycemic control and lipid metabolism in db/db mice. Both interventions modestly reduced body weight, and in leptin receptor–deficient (db/db) mice, treadmill exercise (TE) and WBV restored muscle fiber diameters to within the range of WT mice. Musculo-skeletal loading with TE or WBV reduced adipocyte hypertrophy in visceral fat and attenuated hepatic steatosis. Although effects on bone structure and biomechanics were minimal, TE and WBV both increased circulating levels of osteocalcin in db/db mice. This association, if proven to be causal in subsequent studies, would support the utility of WBV as an exercise mimetic.

Materials and Methods

Animal care, TE, and WBV

Male db/db mice and WT controls on the C57Bl6/J background were obtained from Jackson Laboratories (Bar Harbor, ME) at 5 weeks of age. All animals were housed two per cage

with *ad libitum* access to food and water. Mice from each genotype were assigned to sedentary (SED), WBV, or TE conditions, with each group balanced for an equal distribution of starting weights (n = 14 to 16 per condition). The first week consisted of habituation to the experimental apparatus, followed by 12 weeks of TE or WBV, as previously described (35, 36). In brief, WBV was carried out for 20 minutes per day at a frequency of 32 Hz with $0.5g$ acceleration. TE (Columbus Instruments, Columbus OH) was conducted using a 5% incline at 10 m/min for 45 min/d. Both manipulations were applied daily, with motivation on the treadmill achieved by delivery of compressed air (15 psi) upon noncompliance. TE and WBV began at lights out (18:00) to mimic the active phase of the animals. Mice were weighed weekly throughout the experiment. All procedures followed National Institutes of Health guidelines and were approved by the Institutional Animal Care and Use Committee of the Medical College of Georgia at Augusta University.

Intraperitoneal glucose and insulin tolerance testing

For intraperitoneal glucose tolerance testing (IPGTT), mice were fasted overnight, and preinjection blood samples were rapidly collected from the tail vein within 3 minutes of cage disturbance, as previously described (37). After collecting the first sample, mice were injected with 1.0 g/kg glucose in sterile saline [intraperitoneal (IP)], and postinjection samples were taken at 30, 60, and 120 minutes. Glucose levels in blood samples were determined immediately using a handheld glucometer and Freestyle Lite test strips (Abbott Diabetes Care, Abbott Laboratories, Chicago, IL). For IP insulin tolerance testing, mice were injected with insulin (0.5 IU/kg IP), and postinjection samples were collected at 15 and 60 minutes. Blood glucose was determined using a handheld glucometer as described earlier for IPGTT. Physiological responses to glucose and insulin were quantified using area under the curve (AUC), as previously described (37, 38).

Enzyme-linked immunosorbent assay

To analyze insulin responses to glucose challenge, mice were injected with glucose as described previously for IPGTT, and postinjection blood samples were taken at 30, 60, and 120 minutes. Insulin was quantified in serum samples from each time point using enzyme-linked immunosorbent assay (ELISA) as previously described (37, 39). For ELISA, samples were run in duplicate as specified by the manufacturer (Crystal Chem, Downers Grove, IL) and read at 450 nm on a SpectraMax 384 plate reader (Molecular Devices, Carlsbad, CA). Insulin concentrations were derived from the standard curve using linear regression. Serum osteocalcin was also quantified by ELISA (BT-470; Biomedical Technologies, Stoughton, MA) following manufacturer instructions, as previously described (36).

Serum chemistry and liver function panel

Serum analytes were quantified on a Roche Cobas Fara II robotic chemical analyzer (Risch-Rotkreuz, Switzerland) as previously reported (39, 40). Total cholesterol, triglycerides, and low-density lipoprotein (LDL) were quantified using assay kits from Diagnostic Chemicals Limited (Oxford, CT). High-density lipoprotein was measured using an assay kit from Genzyme Diagnostics (Cambridge, MA). Nonesterified fatty acids (NEFAs) and total ketone bodies (acetoacetone and

3-hydroxybutyrate) were measured using kits from Wako Diagnostics (Richmond, VA). Total ketone bodies (acetoacetone and 3-hydroxybutyrate) were measured using the Total Ketone Bodies Kit (catalog nos. 415-73301 and 411-73401; Wako Diagnostics, Richmond, VA). For the liver function panel, aspartate aminotransferase (AST), alanine transaminase (ALT), gamma glutamyl-transferase (GGT), and total bilirubin were measured using kits from Sekisui Diagnostics (Lexington, MA).

Histology and analysis of hepatic lipids

For adipose tissue histology, the skin was removed from the lower extremities, and the inguinal fat pads were dissected from the subcutaneous region. After bilateral dissection of the inguinal depot, the peritoneal wall was incised to reveal the retroperitoneal fat pads, which were dissected away from the kidney and adrenal. The intrascapular brown adipose depot was excised and weighed after removing any superficial white fat deposits. Fat pad weights were normalized to body weight at euthanasia. Retroperitoneal and inguinal fat pads were subsequently fixed in neutral buffered formalin, paraffin embedded, and stained with hematoxylin and eosin (H&E) staining. Adipocyte diameters were quantified with image analysis software (ImageJ), as previously described (35).

For muscle histology, the soleus and extensor digitorum longus (EDL) muscles were separated along the horizontal plane for paraffin embedding. Paraffin sections were stained with H&E, and minimal fiber diameters were calculated in ImageJ, as previously described (34). To quantify hepatic lipid content, liver samples were weighed, homogenized, and processed for chloroform extraction (41). In brief, samples were homogenized in a 2:1 mixture of methanol:chloroform and treated with a 1:1 mixture of chloroform:KCl. Following centrifugation and desiccation, the extracted lipids were quantified relative to original tissue weight. For histological analysis, liver samples were embedded in optimum cutting temperature (OCT; Sakura Finetek, Torrance, CA) and sectioned on a cryostat (Leica). Slides were subsequently stained with H&E or Oil Red O with hematoxylin counterstaining.

Microcomputed tomography, bone histomorphometry, and biomechanical testing

For analysis of cortical bone architecture, the middiaphysis of each femur was scanned with an *ex vivo* microcomputed tomography system (Skyscan 1174; Bruker microCT, Kontich, Belgium) as previously described (42). Bones were scanned in air using 50 kV, 15-μm isotropic voxels, and 400-ms integration time. Scans were reconstructed and analyzed with SkyScan software to quantify cortical bone thickness (mm), periosteal area (mm^2), cortical bone area (mm^2), and medullary area fraction (%). Analysis of BMD (measured in grams of mineral per square centimeter of tissue) at the femoral neck and femoral middiaphysis was performed using a microcomputed tomography system developed at the Savannah River National Laboratory (Aiken, SC) using 60 kV, 0.148 mA, and 15-μm voxels, as previously described (36).

For histological analysis of bone formation, a subset of mice from each group received two injections of tetracycline (20 mg/kg IP), spaced 10 days apart, immediately prior to euthanasia. The distal third of each tibia was dehydrated, embedded in methyl methacrylate, and sectioned in the horizontal (transverse) plane using a diamond saw, as previously described (43).

Complete images of each tibial cross-section were acquired at 100× final magnification using the Automontage feature in Microlucida software (Microbrightfield, Williston, VT). Analysis of dynamic histomorphometry metrics was carried out for the tibial histology sections as previously described (14), with minor modifications. The endocortical mineral apposition rate was derived from the average distance between double-labeled surfaces divided by the time between tetracycline injections. For biomechanical testing, radii were thawed and placed on steel testing fixtures (5-mm spacing, 2.5 mm on either side of center). Testing was carried out by linear displacement at 0.10 mm/s using a Transducer Techniques 5-kg load cell, with data recorded every 0.01 seconds. Bones were loaded to failure, and ultimate load and stiffness (slope) were calculated from the load-displacement curves, as previously reported (36).

Statistics

Measures of liver, muscle, and adipose tissue were analyzed using 2 × 3 analysis of variance (ANOVA) designs, with genotype (WT × db/db) and intervention (SED × WBV × TE) as fixed factors. When statistically significant ($P < 0.05$) effects of intervention were observed, we conducted within-genotype comparisons using one-way ANOVA, followed by *post hoc* comparison of each intervention group with genotype-matched SED mice using Bonferroni-corrected *t* tests. Body weights over the course of the experiment were compared across groups and treatment conditions using 2 × 3 repeated measures ANOVA, followed by *post hoc* testing as described previously. For IPGTT and IP insulin tolerance testing data sets, AUC was computed and compared across groups using 2 × 3 ANOVA followed by *post hoc* comparisons as described earlier for single–end point measures. Statistics were performed in PASW Statistics version 11 (IBM Corporation, Armonk, NY), and graphs were generated using Graphpad Prism 5.0 (Graphpad, La Jolla, CA).

Results

Exercise and WBV reduce weight gain and muscle atrophy in db/db mice

Twelve weeks of daily TE or WBV reduced weight gain in db/db and WT mice [Fig. 1(a–d); effect of intervention, $F_{2,36} = 5.81, P < 0.01$]. Although all groups of db/db mice weighed significantly more than WT mice [Fig. 1(a–d); effect of genotype, $F_{1,36} = 76.55, P < 0.001$], db/db mice exposed to TE weighed significantly less than SED db/db mice at the end of the experiment [Fig. 1(d); *post hoc* comparison, db/db SED vs db/db WBV, not significant ; db/db SED vs db/db TE, $t_{14} = 3.75, P < 0.01$]. The modest reductions in weight gain observed with TE and WBV may have been attributable to muscle hypertrophy, as db/db mice responded to these interventions with significant increases in EDL fiber diameter [Fig. 1(e) and 1(f); effect of intervention in db/db, $F_{2,18} = 8.84, P < 0.05$; *post hoc* comparison, db/db SED vs db/db WBV, $t_{13} = 3.93, P < 0.01$; db/db SED vs db/db TE, $t_{11} = 3.28, P < 0.01$]. Similar trends were observed in the soleus, although these effects did not reach statistical significance [Fig. 1(g)]. These results demonstrate that exercise and WBV
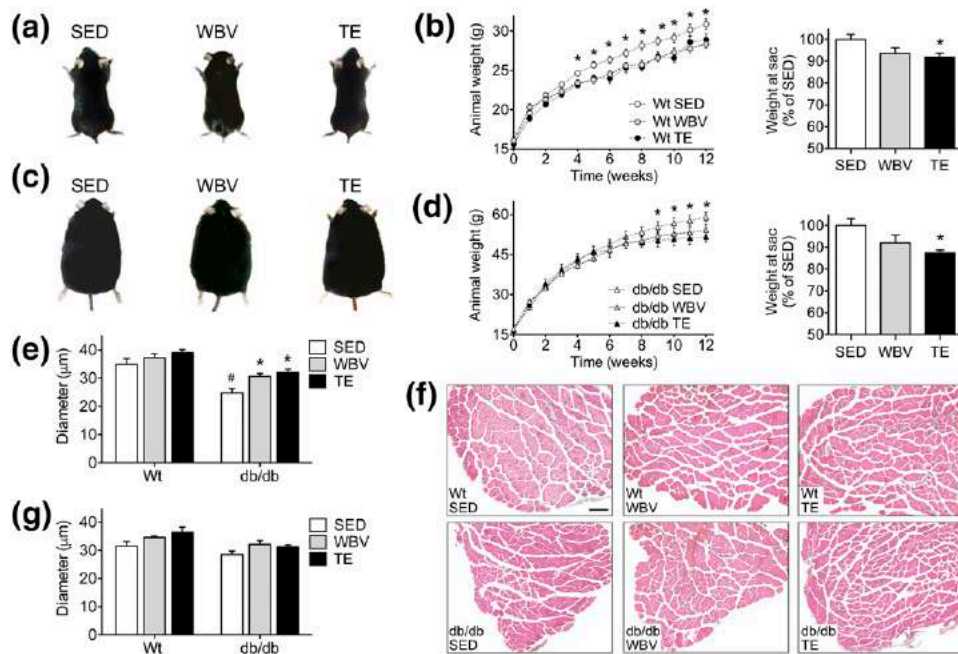
Figure 1. Musculoskeletal loading reduces weight gain and attenuates muscle atrophy in db/db mice. (a) Representative images of WT gross morphology after 3 months of SED conditions, WBV, or TE. (b) Both interventions reduced weight gain in WT mice (left), and analysis of body weight at euthanasia relative to WT SED mice revealed statistically significant reductions after exercise (right). (c) Representative images of db/db morphology after 3 months of each intervention. (d) Exercise and WBV reduced weight gain over the final month of the experiment in db/db mice (left), and TE significantly reduced body weight relative to db/db SED mice at euthanasia (right). (e) Exercise and WBV prevent muscle fiber atrophy in the EDL of db/db mice. (f) Micrographs show representative images of H&E staining in EDL samples from the indicated groups. Scale bar = 100 μm. (g) There was no significant effect of TE or WBV on muscle fiber diameter in the soleus. For graphs, bars and symbols represent the average of (n = 6 to 8) mice in the indicated conditions, and hashtags denote the effect of genotype following 2 × 3 ANOVA with statistical significance at $P < 0.05$. Asterisks indicate significant differences relative to matched-genotype SED mice following repeated-measures ANOVA (b, d) or one-way ANOVA with Bonferroni-corrected *post hoc* comparisons (e, g).

normalize muscle fiber diameter in db/db mice. Because muscle hypertrophy was coincident with small but significant reductions in weight gain, exercise and WBV exert similar effects on body composition in leptin receptor–deficient mice.

Physical activity and WBV attenuate adipocyte hypertrophy in visceral fat

Consistent with their obese phenotype, db/db mice had significantly more visceral white adipose tissue (vWAT), based on comparisons of retroperitoneal fat pad weights relative to body weights at euthanasia [Fig. 2(a); effect of genotype, $F_{1,42} = 55.84, P < 0.01$]. db/db mice also exhibit significantly greater subcutaneous adiposity, based on analysis of inguinal fat pad weights relative to body weight [Fig. 2(b); effect of genotype, $F_{1,42} = 48.27, P < 0.01$]. The ratio of intrascapular brown adipose tissue to body weight was also significantly greater in db/db mice [Fig. 2(c); effect of genotype, $F_{1,42} = 19.79, P < 0.01$].

Quantification of adipocyte morphology in vWAT revealed that musculoskeletal loading significantly reduced cellular hypertrophy in db/db mice [Fig. 2(d); effect of intervention in db/db, $F_{2,18} = 32.91, P < 0.01$]. Both TE and WBV reduced the diameter of vWAT adipocytes in db/db mice relative to db/db SED [Fig. 2(e); *post hoc*

comparison, db/db SED vs db/db WBV, $t_{14} = 5.14, P < 0.01$; db/db SED vs db/db TE, $t_{16} = 7.08, P < 0.01$]. These effects were observed in vWAT, but not in subcutaneous white adipose tissue, where all groups of db/db mice exhibit similar degrees of adipocyte hypertrophy relative to WT mice [Fig. 2(f); effect of genotype, $F_{1,30} = 17.52, P < 0.01$]. When interpreted alongside of increases in muscle fiber diameter [Fig. 1(e)], attenuation of vWAT adipocyte hypertrophy provides further evidence for repartitioning of body composition after musculoskeletal loading in db/db mice.

Musculoskeletal loading enhances glycemic control and insulin sensitivity in db/db mice

db/db mice exhibit fasting hyperglycemia, based on comparison of serum glucose levels taken before IPGTT [Fig. 3(a) and 3(b)]. TE reduced circulating glucose levels at 60 and 120 minutes after glucose challenge [Fig. 3(a); effect of intervention in db/db, $F_{2,18} = 8.61, P < 0.05$]. The effect of TE in db/db mice was statistically significant following comparison of the AUC [Fig. 3(b); *post hoc* comparison, db/db SED vs db/db WBV, NS; db/db SED vs db/db TE, $t_{11} = 3.09, P < 0.05$]. Similar trends were observed for the effect of TE in WT mice, but these did not reach statistical significance [Fig. 3(a)]. These results indicate that TE enhances glucose clearance in leptin receptor mutant mice.
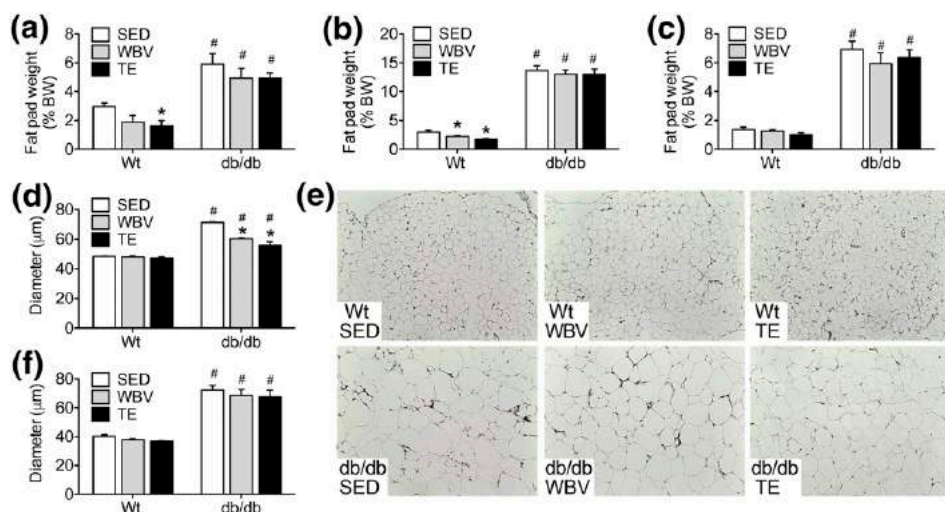
Figure 2. TE and WBV comparably attenuate adipocyte hypertrophy in visceral fat from db/db mice. (a) db/db mice exhibit significantly greater visceral adiposity than WT mice based on increases in the weight of the retroperitoneal fat pads after dissection and normalization to body weight (BW) at euthanasia. (b) db/db mice also exhibit increases in subcutaneous adiposity relative to WT mice based on the ratio of inguinal fat pad weights to body weight. (c) The proportional weight of intrascapular brown fat was also greater in db/db mice relative to WT mice. (d) TE or WBV reduced adipocyte diameter in retroperitoneal fat relative to SED db/db mice. (e) Micrographs show representative H&E staining of retroperitoneal fat from mice in the indicated conditions. Scale bar = 200 μm. (f) Adipocyte hypertrophy in subcutaneous fat was unaffected by TE or WBV in db/db mice. For graphs, bars represent the average of (n = 6 to 8) mice in the indicated conditions, and hashtags denote the effect of genotype following 2 × 3 ANOVA with statistical significance at $P < 0.05$. Asterisks indicate significant differences relative to matched-genotype SED mice following one-way ANOVA with Bonferroni-corrected *post hoc* comparisons.

Analysis of serum insulin levels before and after glucose challenge revealed parallel effects of TE and WBV in db/db mice. SED db/db mice exhibit elevated fasting insulin levels, but TE and WBV comparably reduced insulin concentrations in samples taken prior to glucose administration [Fig. 3(c); effect of intervention in db/db, $F_{2,18} = 6.71$, $P < 0.05$]. Similar trends were observed following analysis of the AUC, which revealed significant reductions in insulin responses to glucose challenge after TE or WBV in db/db mice [Fig. 3(c); *post hoc* comparison, db/db SED vs db/db WBV, $t_{11} = 7.82$, $P < 0.01$; db/db SED vs db/db TE, $t_{11} = 10.91$, $P < 0.01$]. As expected given the low intensity of the loading interventions, there was no effect of TE or WBV on insulin responses to glucose challenge in WT mice [Fig. 3(c)]. This outcome suggests that TE and WBV may enhance pancreatic sensitivity to glucose in db/db mice.

To directly examine insulin sensitivity, we examined changes in circulating glucose following insulin administration in WT and db/db mice exposed to TE, WBV, or SED conditions. SED db/db mice were unresponsive to insulin, but TE and WBV partially restored insulin sensitivity [Fig. 3(e); effect of intervention in db/db, $F_{2,16} = 4.96$, $P < 0.05$]. These effects were also reflected by the AUC, which was significantly reduced in db/db mice exposed to TE or WBV, relative to SED db/db mice [Fig. 3(f); *post hoc* comparison, db/db SED vs db/db WBV, $t_{11} = 3.33$, $P < 0.05$; db/db SED vs db/db TE, $t_{11} = 6.93$, $P < 0.01$]. All groups of WT mice exhibited similar reductions in serum glucose after insulin administration,

indicating that there was no effect of TE or WBV on insulin sensitivity in WT mice [Fig. 3(e) and 3(f)]. Taken together, these results indicate that TE and WBV exert similar effects on glucose metabolism and insulin sensitivity in db/db mice.

TE and WBV attenuate hepatic steatosis in db/db mice

Significant increases in hepatic lipid content are exhibited in db/db mice relative to WT mice [Fig. 4(a); effect of genotype, $F_{1,38} = 18.27$, $P < 0.01$]. In db/db mice, TE and WBV significantly reduced hepatic lipids [Fig. 4(a); effect of intervention in db/db, $F_{2,20} = 14.57$, $P < 0.01$; *post hoc* comparison, db/db SED vs db/db WBV, $t_{13} = 4.13$, $P < 0.01$; db/db SED vs db/db TE, $t_{11} = 3.72$, $P < 0.01$]. Although the effects were less dramatic than in db/db mice, WT mice also responded to TE and WBV with reductions in hepatic lipid content, but these did not reach statistical significance in *post hoc* comparisons [Fig. 4(a)]. Histological examination of H&E staining in liver sections revealed widespread evidence of hepatic steatosis in db/db mice relative to WT mice [Fig. 4(b)]. Consistent with the quantitative data from liver lipid extraction, WBV and TE only partially reduced Oil Red O staining in db/db mice, as differences were still visually apparent upon comparison with liver sections from WT mice [Fig. 4(b)].

Mild hepatomegaly also occurred in db/db mice, based on significant increases in liver weights relative to body weight following comparison with WT mice [Fig. 4(c);
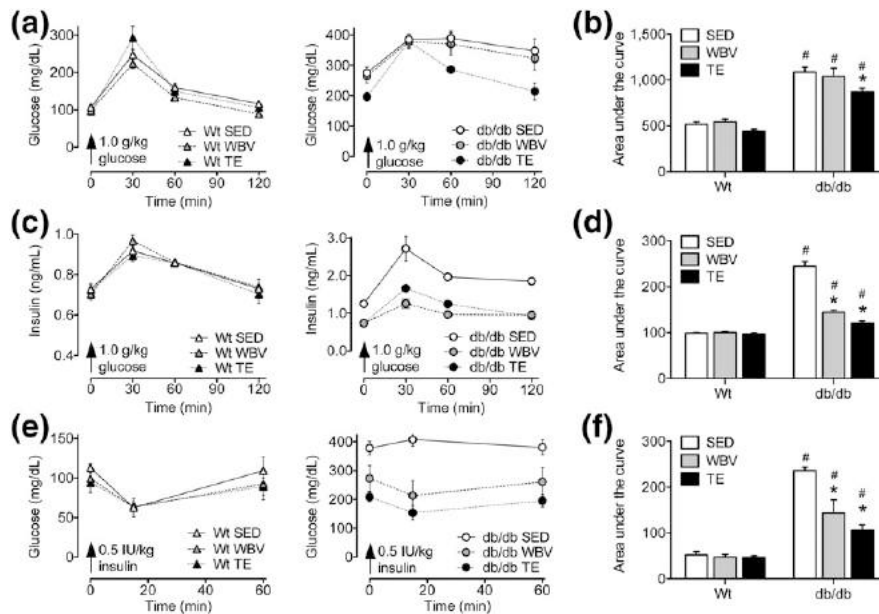
Figure 3. Partial reinstatement of glycemic control and recovery of insulin sensitivity following exercise or WBV in db/db mice. (a) Left graph shows fasting glucose levels and responses to IP glucose administration in WT mice exposed to TE, WBV, or SED conditions. Right graph shows fasting glucose and responses to IPGTT in db/db mice. (b) Bars represent group averages for the AUC, which was computed using serum glucose values taken before and at intervals after IP glucose challenge. Exercise reduces the AUC in db/db mice relative to db/db SED mice, indicative of enhanced glucose clearance. (c) Left graph shows fasting insulin levels and insulin responses to IP glucose in WT mice, and right graph shows measures from db/db mice in the indicated conditions. (d) In db/db mice, exercise and WBV reduced AUC values derived from insulin responses to glucose challenge. Reductions in AUC relative to db/db SED mice are indicative of enhanced pancreatic sensitivity to glucose after musculoskeletal loading. (e) Left graph shows serum glucose levels before and after IP insulin administration in WT mice, and right graph shows these measures for the indicated groups of db/db mice. (f) Comparison of the AUC from glucose responses to insulin challenge revealed that exercise and WBV partially restored insulin sensitivity in db/db mice relative to db/db SED mice. Although all groups of db/db mice were insulin resistant relative to WT mice, the reductions observed following exercise and WBV suggest enhancement of insulin sensitivity. For graphs, bars and symbols represent the average of (n= 6 to 8) mice in the indicated conditions, and hashtags denote the effect of genotype following 2×3 ANOVA with statistical significance at $P < 0.05$. Asterisks indicate significant differences relative to matched-genotype SED mice following one-way ANOVA with Bonferroni-corrected *post hoc* comparisons.

effect of genotype, $F_{1,39} = 60.41$, $P < 0.01$]. In serum samples, db/db mice had higher concentrations of ALT [Fig. 4(d); effect of genotype, $F_{1,39} = 84.55$, $P < 0.01$], with no change in levels of AST [Fig. 4(e)]. There was no effect of genotype or intervention on levels of GGT, but the change in AST/ALT ratio observed in db/db mice indicates that reductions in hepatic lipids with exercise or WBV represent a partial, rather than total, normalization of liver function. This interpretation is also supported by analysis of serum lipids, which revealed significant increases in cholesterol (effect of genotype, $F_{1,71} = 13.73$, $P < 0.01$), LDL (effect of genotype, $F_{1,35} = 95.57$, $P < 0.01$), triglycerides (effect of genotype, $F_{1,68} = 45.83$, $P < 0.01$), NEFAs (effect of genotype, $F_{1,38} = 6.09$, $P < 0.05$), and total ketone bodies (effect of genotype, $F_{1,35} = 4.58$, $P < 0.05$) in db/db mice (Table 1). These observations indicate that dyslipidemia in db/db mice persists after the musculoskeletal loading protocols used in these experiments.

Regional differences in skeletal responses to musculoskeletal loading in db/db mice

SED db/db mice had significantly lower circulating osteocalcin levels than WT mice [Fig. 5(a); effect of

genotype, $F_{1,57} = 63.53$, $P < 0.01$]. Musculoskeletal loading with TE or WBV increased serum osteocalcin in db/db mice relative to SED db/db mice (effect of intervention in db/db, $F_{2,35} = 17.02$, $P < 0.01$; *post hoc* comparison, db/db SED vs db/db WBV, $t_{22} = 5.46$, $P < 0.01$; db/db SED vs db/db TE, $t_{22} = 5.93$, $P < 0.01$). Neither manipulation restored serum osteocalcin to the levels observed in WT mice, but the increase relative to SED db/db mice indicates that musculoskeletal loading exerts effects on the skeleton, even in the context of leptin receptor deficiency. Although serum osteocalcin levels increased following musculoskeletal loading in db/db mice, quantification of the endocortical mineral apposition rate in the tibial diaphysis revealed no effect of genotype or musculoskeletal loading [Fig. 5(b)]. db/db mice exhibit reductions in cortical bone area in the femur (effect of genotype, $F_{1,39} = 38.01$, $P < 0.01$), but cortical bone loss was unaffected by either intervention [Fig. 5(c)]. Similar genotype effects were evident upon comparisons of the periosteal area of the femur, which was significantly reduced in db/db mice [Fig. 5(d); effect of genotype, $F_{1,39} = 23.96$, $P < 0.01$]. Although there was a trend for increases in periosteal area after TE in db/db mice, this
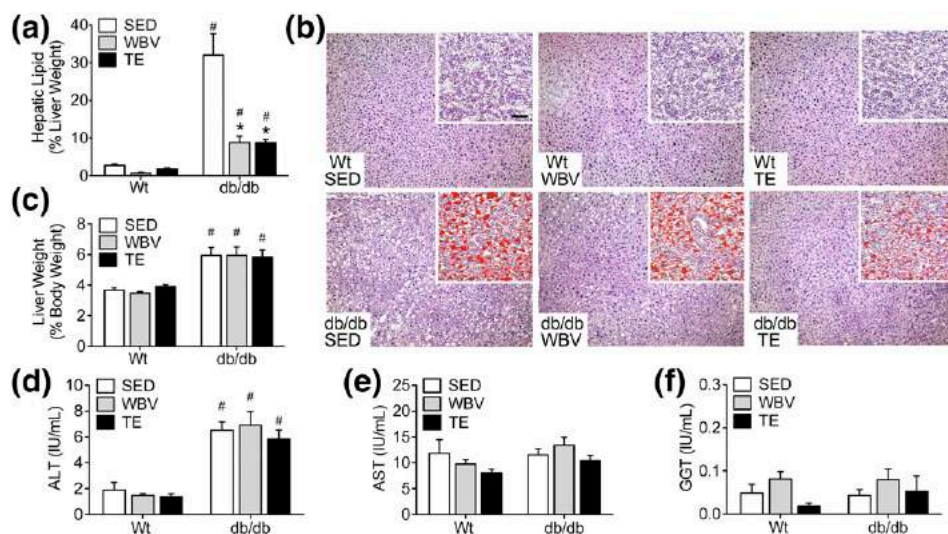
Figure 4. Musculoskeletal loading decreases hepatic lipid content in db/db mice. (a) Three months of daily TE or WBV reduced hepatic lipid content in db/db mice relative to SED db/db mice. (b) Similar effects were observed in liver cryosections stained with H&E (micrographs) or Oil Red O with hematoxylin counterstaining (inset). (c) db/db mice exhibit liver hypertrophy based on analysis of hepatic weight relative to body weight at euthanasia. (d) db/db mice also had higher circulating concentrations of ALT relative to WT mice. (e) There was no effect of genotype or intervention on levels of AST in serum samples. (f) There was no effect of genotype or intervention on levels of GGT. For graphs, bars represent the average of (n = 6 to 8) mice in the indicated conditions, and hashtags denote the effect of genotype following 2 × 3 ANOVA with statistical significance at $P < 0.05$. Asterisks indicate significant differences relative to matched-genotype SED mice following one-way ANOVA with Bonferroni-corrected *post hoc* comparisons.

did not reach statistical significance [Fig. 5(d); for effect of intervention in db/db, $F_{2,18} = 2.85$, $P = 0.08$].

Micro–computed tomography (microCT) analysis revealed that db/db mice exhibit reduced BMD in the femoral neck, relative to WT mice [Fig. 6(a); effect of genotype, $F_{1,38} = 19.67$, $P < 0.01$]. TE, but not WBV, normalized BMD in db/db mice [Fig. 6(a); effect of intervention in db/db, $F_{1,20} = 15.12$, $P < 0.01$; *post hoc* comparison, db/db SED vs db/db WBV, NS; db/db SED vs db/db TE, $t_{11} = 3.86$, $P < 0.01$]. These effects were regionally differentiated along the length of the femur, as midshaft BMD was unaffected by genotype or musculoskeletal loading [Fig. 6(b)]. Biomechanical testing in the radius revealed that db/db mice had significantly reduced bone strength, as measured by ultimate load, compared with WT mice [Fig. 6(c); effect of genotype, $F_{1,53} = 25.28$, $P < 0.01$]. However, neither of the interventions had a significant impact on bone strength relative to matched-genotype SED mice [Fig. 6(c)]. Likewise, radial stiffness

was not significantly impacted by genotype or experimental condition [Fig. 6(d)]. In the context of increased serum osteocalcin, the modest effects of TE and WBV on bone geometry, mineralization, and biomechanics may reflect distributed osteogenic responses in multiple areas of the skeleton.

Discussion

In this report, we compared the metabolic and osteogenic effects of WBV with the effects of TE in a mouse model of genetic obesity and diabetes (db/db mice). We found that TE and WBV exert similar effects on muscle fiber diameter in db/db mice. SED db/db mice exhibited muscle atrophy, but TE and WBV restored muscle fiber diameter to within the range of WT mice. Exercise and WBV reduced adipocyte hypertrophy in visceral fat, attenuated hepatic steatosis, and enhanced glycemic control in db/db mice. Although skeletal responses to

Table 1.   Serum Biochemistry

	WT/SED	WT/WBV	WT/TE	db/db SED	db/db WBV	db/db TE
Total cholesterol	120 ± 15.9	132 ± 12.8	110 ± 13.1	190 ± 30.5[a]	189 ± 29.1[a]	194 ± 31.5[a]
LDL	39 ± 5.4	36 ± 2.6	27 ± 3.1	137 ± 17.8[a]	125 ± 22.1[a]	126 ± 7.0[a]
Triglycerides	84 ± 10.1	94 ± 6.3	76 ± 7.8	172 ± 18.8[a]	148 ± 14.6[a]	130 ± 9.7[a]
NEFAs	1113 ± 84.5	1201 ± 75.8	1079 ± 48.2	1259 ± 113.3[a]	1402 ± 182.8[a]	1632 ± 313.5[a]
Ketones	229 ± 21.3	266 ± 21.8	281 ± 41.7	364 ± 57.1[a]	373 ± 48.4[a]	243 ± 16.5[a]

Means ± standard error of the mean are shown.

[a]The effect of genotype following 2 × 3 ANOVA with statistical significance at $P < 0.05$.
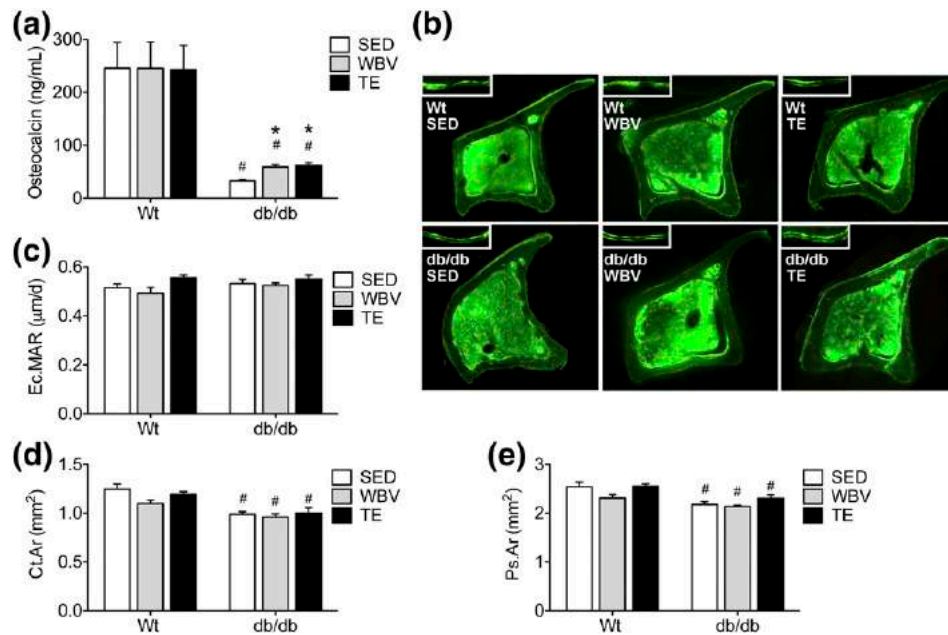
Figure 5. Exercise and WBV increase serum osteocalcin levels in db/db mice. (a) TE and WBV increase serum osteocalcin in db/db mice relative to SED db/db mice. (b) Micrographs show representative montages of tetracycline labeling in tibial cross-sections from the indicated groups. Scale bar = 200 μm. Insets show labeled surfaces visualized after two injections of tetracycline, with 10 days between injections. (c) Analysis of endocortical mineral apposition rates (Ec.MARs) in tibial cross-sections revealed no significant effect of genotype or intervention. (d) db/db mice exhibit reductions in cortical bone area (Ct.Ar) as determined by microCT analysis in the femur. (e) Leptin receptor deficiency reduces the periosteal area (Ps.Ar) in femur samples, as determined by microCT. For graphs, bars represent the average of (n = 6 to 8) mice in the indicated conditions, and hashtags denote the effect of genotype following 2 × 3 ANOVA with statistical significance at $P < 0.05$. Asterisks indicate significant differences relative to matched-genotype SED mice following one-way ANOVA with Bonferroni-corrected *post hoc* comparisons.

exercise and WBV were modest, the increases in serum osteocalcin suggest that db/db mice exhibit osteogenic responses to both interventions. Taken together, these findings demonstrate that WBV recapitulates the effects of exercise on metabolism in a mouse model of obesity and insulin resistance.

Two recently published reports by independent groups have shown that WBV attenuates fasting hyperglycemia and hyperinsulinemia in db/db mice (44, 45). However, these reports did not incorporate kinetic analyses to investigate potential tissue-specific alterations in insulin sensitivity and glucose metabolism. We observed that
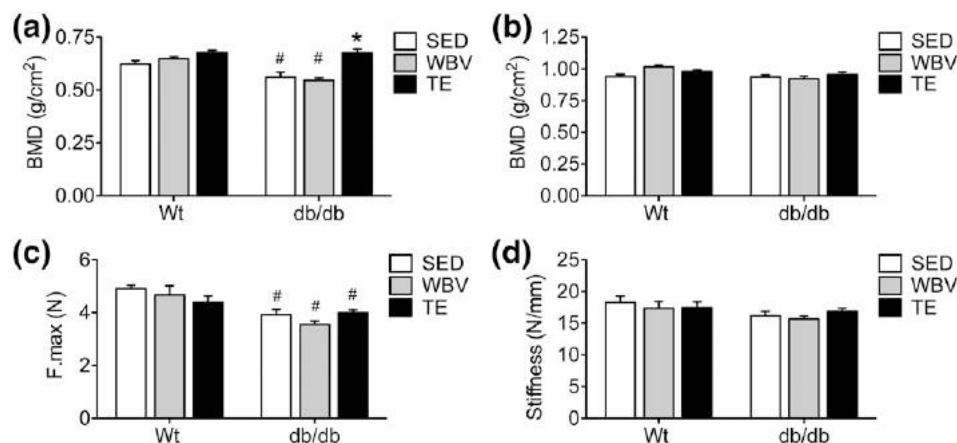

Figure 6. Exercise and WBV enhance cortical BMD in db/db mice. (a) Three months of daily TE increased BMD at the femoral neck in db/db mice. (b) The effects of genotype were regionally differentiated along the length of the femur, as BMD at the femoral middiaphysis was similar between WT and db/db mice. (c) Biomechanical analysis of ultimate load (F.Max) in the radius revealed reductions in bone strength in db/db mice. (d) There were no effects of genotype or musculoskeletal loading on stiffness (N/mm) following biomechanical testing in the radius. For graphs, bars represent the average of (n = 6 to 8) mice in the indicated conditions, and hashtags denote the effect of genotype following 2 × 3 ANOVA with statistical significance at $P < 0.05$. Asterisks indicate significant differences relative to matched-genotype SED mice following one-way ANOVA with Bonferroni-corrected *post hoc* comparisons.

WBV partially normalizes pancreatic responses to glucose, based on analysis of serum insulin responses to glucose challenge. WBV also rescued insulin sensitivity, based on reductions in serum glucose after insulin administration. Exercise and WBV exert comparable effects on insulin sensitivity and pancreatic responses to glucose, but WBV did not recapitulate the effects of exercise on glucose clearance in db/db mice. Understanding the kinetics and tissue-specific loci for responses to exercise and WBV is critical to inform the timing and modality of both interventions in future studies.

Findings from rodent models of obesity have shown that WBV attenuates dyslipidemia (45, 46). In aged mice and rodents with diet-induced obesity, WBV reduced adiposity and lowered serum triglycerides (47–49), but the magnitude of these effects had never been examined relative to exercise. We observed comparable reductions in adipocyte diameter following TE or WBV in leptin receptor–deficient mice. Although this effect was not accompanied by changes in serum triglycerides, it is noteworthy that db/db mice retained physiological responses to musculoskeletal loading despite severe and widespread metabolic deficits. The reductions in hepatic lipid content and steatosis observed following WBV in male db/db mice in the current study are also consistent with a recent report in female db/db mice (45). Liu et al. (45) demonstrated that the hepatic effects of WBV were correlated with reductions in sterol regulatory element binding protein 1c (SREBP1c), a transcription factor that regulates genes involved in cholesterol metabolism (50). Although it is possible that the effects of WBV on glycemic control and hepatic lipids might be mediated by a shared mechanism, this possibility remains speculative and will require targeted manipulation of SREBP1c and other pathways associated with WBV effects on the liver.

Previous work in rodent models indicates that WBV attenuates muscle atrophy with disuse and aging and in experimental models of menopause (23, 51–53). Leptin-deficient mice exhibit widespread reductions in muscle fiber diameter and cellularity (14, 54). Loss of skeletal muscle in models of leptin deficiency has been linked with imbalances between hypertrophic and atrophic myokines (34, 55–57). There are interesting similarities between the results of the current study and published data from leptin-deficient mice with genetic ablation of the atrophic hormone myostatin (55, 56). Specifically, the metabolic effects of musculoskeletal loading in the current experiments resemble the partial restoration of insulin sensitivity reported in leptin-deficient mice following myostatin ablation (55, 56). It is therefore possible that changes in secreted factors from skeletal muscle could be contributing to the effects of exercise and WBV. This possibility is not exclusive to myostatin, because the cytokine interleukin-6 (IL-6) also plays a critical role in exercise-induced muscle hypertrophy, and the secreted hormone irisin is released in response to exercise and promotes energy expenditure (57). The effects of exercise and WBV on muscle atrophy and metabolic dysfunction in the current data set may also be mediated by dissociable mechanisms. Future studies will be required to examine whether physical activity and WBV promote muscle hypertrophy via a common mechanism and to elucidate the role of myokines in the metabolic effects of loading interventions.

Although the effects of leptin deficiency on bone remain controversial, decreases in cortical bone mass in weight-bearing regions of the skeleton like the tibia and femur represent the most consistently reported skeletal phenotype in leptin-deficient rodents (12–16, 52). Recently published findings suggest that WBV increases trabecular and cortical bone mass in db/db mice (44), but these effects differ from the modest skeletal responses observed after exercise and WBV in the current study. The differential outcomes could be attributable to the greater intensity and duration of the WBV protocol used by Jing et al. (44); specifically, this report applied comparable mechanical force (0.5 g) at slightly higher frequency (45 Hz, as opposed to 32 Hz in the current study). The duration (20 minutes) used in the current study was based on previous work by our group demonstrating attenuation of age-related bone loss in male mice (36), but this duration is also less than the 60-minute protocol shown to promote bone formation in the study by Jing et al. (44). The dose dependency of WBV effects on bone formation and metabolism warrant further study, and the different outcomes observed at the skeletal level may be explained by methodological differences. However, our observation that WBV increases serum osteocalcin in db/db mice is consistent with the findings of Jing et al. (44). Because the increases in osteocalcin observed in the current study were comparable to those evoked by treadmill training, our results demonstrate that WBV elicits replicable increases in osteocalcin that recapitulate the effects of exercise.

As noted previously (12, 16), SED db/db mice in the current study had lower circulating osteocalcin levels than SED WT mice. TE and WBV increased circulating osteocalcin in db/db mice, relative to SED db/db mice, but did not restore levels to within the range of WT mice. Although the metabolic effects of osteocalcin are still being elucidated (58, 59), several studies suggest that undercarboxylated osteocalcin regulates glycemic control and lipid metabolism in mouse models (27, 30, 60). Osteocalcin-deficient mice exhibit insulin resistance and hyperglycemia (27), and administration of undercarboxylated osteocalcin protects against the metabolic

consequences of diet-induced obesity in WT mice (30, 60). In the present studies, the effects of musculoskeletal loading on serum osteocalcin in db/db mice were correlated with improvements in glycemic control and insulin sensitivity, but it is important to note that total, rather than undercarboxylated, osteocalcin was measured here. Although the metabolic responses observed are consistent with the cellular consequences of osteocalcin exposure in pancreatic β-cells and myoblasts *in vitro* (27–29, 61), the metabolic effects of exercise and WBV may not be dependent on osteocalcin *per se*. Serum osteocalcin reflects global bone formation (27, 28), and osteoblasts can regulate metabolism in an osteocalcin-independent manner (59, 62). Direct manipulation of osteocalcin will be required to determine whether increases are required for enhanced glycemic control with exercise and WBV.

Although comparisons across published findings in the human literature reveal broad similarities between the metabolic effects of exercise and WBV, there have been no direct comparisons of these interventions. Both forms of musculoskeletal loading attenuate obesity, insulin resistance, and sarcopenia in humans (19, 20, 25, 63–65), but differences in patient population characteristics and the methods used to evaluate metabolism prevent analysis of the relative efficacy of WBV relative to exercise. In any case, the transferability of the current results to humans would require preliminary demonstration of similar outcomes in outbred animal models, as the inbred strains used in these experiments exhibit greater genetic homogeneity than human populations. Conducting genome-wide association studies in an outbred animal model could potentially identify predictive loci for comparable metabolic responses to exercise and WBV. If genetic predictors of sensitivity to exercise and WBV were conserved in humans, it might be possible to use single nucleotide polymorphisms or other genetic covariates as biomarkers to identify populations likely to benefit from WBV. The primary conclusion drawn from the current report is that WBV recapitulates some of the metabolic effects of exercise in mice with genetic obesity and diabetes. Future studies will focus on comparing the effects of musculoskeletal loading in outbred models, but in the human literature, it would be beneficial to consider direct comparisons of WBV with exercise interventions. With the increasing prevalence of obesity and its comorbidities, WBV warrants further investigation as a strategy to attenuate risk factors for cardiovascular and metabolic diseases.

Acknowledgments

Address all correspondence and requests for reprints to: Alexis M. Stranahan, PhD, Department of Neuroscience and Regenerative Medicine, Medical College of Georgia, Augusta University, 1120 15th Street, Augusta, Georgia 30912. E-mail: astranahan@augusta.edu.

References

1. Felson DT, Zhang Y, Hannan MT, Anderson JJ. Effects of weight and body mass index on bone mineral density in men and women: the Framingham study. *J Bone Miner Res*. 1993;**8**(5):567–573.
2. Zaidi M, Buettner C, Sun L, Iqbal J. Minireview: the link between fat and bone: does mass beget mass? *Endocrinology*. 2012;**153**(5):2070–2075.
3. Bini V, Igli Baroncelli G, Papi F, Celi F, Saggese G, Falorni A. Relationships of serum leptin with biochemical markers of bone turnover and with growth factors in normal weight and overweight children. *Horm Res*. 2004;**61**(4):170–175.
4. Yamamoto M, Yamaguchi T, Nawata K, Yamauchi M, Sugimoto T. Decreased PTH levels accompanied by low bone formation are associated with vertebral fractures in postmenopausal women with type 2 diabetes. *J Clin Endocrinol Metab*. 2012;**97**(4):1277–1284.
5. Manavalan JS, Cremers S, Dempster DW, Zhou H, Dworakowski E, Kode A, Kousteni S, Rubin MR. Circulating osteogenic precursor cells in type 2 diabetes mellitus. *J Clin Endocrinol Metab*. 2012;**97**(9):3240–3250.
6. Rubin MR. Bone cells and bone turnover in diabetes mellitus. *Curr Osteoporos Rep*. 2015;**13**(3):186–191.
7. Adler BJ, Kaushansky K, Rubin CT. Obesity-driven disruption of haematopoiesis and the bone marrow niche. *Nat Rev Endocrinol*. 2014;**10**(12):737–748.
8. Kanneganti TD, Dixit VD. Immunological complications of obesity. *Nat Immunol*. 2012;**13**(8):707–712.
9. Thomas T, Gori F, Khosla S, Jensen MD, Burguera B, Riggs BL. Leptin acts on human marrow stromal cells to enhance differentiation to osteoblasts and to inhibit differentiation to adipocytes. *Endocrinology*. 1999;**140**(4):1630–1638.
10. Scheller EL, Song J, Dishowitz MI, Soki FN, Hankenson KD, Krebsbach PH. Leptin functions peripherally to regulate differentiation of mesenchymal progenitor cells. *Stem Cells*. 2010;**28**(6):1071–1080.
11. Sasaki T, Kuroko M, Sekine S, Matsui S, Kikuchi O, Susanti VY, Kobayashi M, Tanaka Y, Yuasa T, Kitamura T. Overexpression of insulin receptor partially improves obese and diabetic phenotypes in db/db mice. *Endocr J*. 2015;**62**(9):787–796.
12. Mathey J, Horcajada-Molteni MN, Chanteranne B, Picherit C, Puel C, Lebecque P, Cubizoles C, Davicco MJ, Coxam V, Barlet JP. Bone mass in obese diabetic Zucker rats: influence of treadmill running. *Calcif Tissue Int*. 2002;**70**(4):305–311.
13. Ealey KN, Fonseca D, Archer MC, Ward WE. Bone abnormalities in adolescent leptin-deficient mice. *Regul Pept*. 2006;**136**(1-3):9–13.
14. Hamrick MW, Pennington C, Newton D, Xie D, Isales C. Leptin deficiency produces contrasting phenotypes in bones of the limb and spine. *Bone*. 2004;**34**(3):376–383.

15. Turner RT, Kalra SP, Wong CP, Philbrick KA, Lindenmaier LB, Boghossian S, et al. Peripheral leptin regulates bone formation. *J Bone Miner Res*. 2013;**28**(1):22–34.

16. Williams GA, Callon KE, Watson M, Costa JL, Ding Y, Dickinson M, Wang Y, Naot D, Reid IR, Comish J. Skeletal phenotype of the leptin receptor-deficient db/db mouse. *J Bone Miner Res*. 2011;**26**(8):1698–1709.

17. Warden SJ, Mantila Roosa SM, Kersh ME, Hurd AL, Fleisig GS, Pandy MG, Fuchs RK. Physical activity when young provides lifelong benefits to cortical bone size and strength in men. *Proc Natl Acad Sci USA*. 2014;**111**(14):5337–5342.

18. Alfonso-Rosa RM, Del Pozo-Cruz J, Del Pozo-Cruz B, Sañudo B, Abellán-Perpiñán JM. Cost-utility analysis of a 12-week whole-body vibration based treatment for people with type 2 diabetes: reanalysis of a RCT in a primary care context. *Public Health*. 2015;**129**(7):993–995.

19. del Pozo-Cruz B, Alfonso-Rosa RM, del Pozo-Cruz J, Sañudo B, Rogers ME. Effects of a 12-wk whole-body vibration based intervention to improve type 2 diabetes. *Maturitas*. 2014;**77**(1):52–58.

20. Erceg DN, Anderson LJ, Nickles CM, Lane CJ, Weigensberg MJ, Schroeder ET. Changes in bone biomarkers, BMC, and insulin resistance following a 10-week whole body vibration exercise program in overweight Latino boys. *Int J Med Sci*. 2015;**12**(6):494–501.

21. Rubin C, Turner AS, Bain S, Mallinckrodt C, McLeod K. Anabolism. Low mechanical signals strengthen long bones. *Nature*. 2001;**412**(6847):603–604.

22. Xie L, Rubin C, Judex S. Enhancement of the adolescent murine musculoskeletal system using low-level mechanical vibrations. *J Appl Physiol*. 2008;**104**(4):1056–1062.

23. Judex S, Lei X, Han D, Rubin C. Low-magnitude mechanical signals that stimulate bone formation in the ovariectomized rat are dependent on the applied frequency but not on the strain magnitude. *J Biomech*. 2007;**40**(6):1333–1339.

24. Judex S, Zhong N, Squire ME, Ye K, Donahue LR, Hadjiargyrou M, Rubin CT. Mechanical modulation of molecular signals which regulate anabolic and catabolic activity in bone tissue. *J Cell Biochem*. 2005;**94**(5):982–994.

25. Rubin C, Judex S, Qin YX. Low-level mechanical signals and their potential as a non-pharmacological intervention for osteoporosis. *Age Ageing*. 2006;**35**(Suppl 2):ii32–ii36.

26. Rubin C, Turner AS, Mallinckrodt C, Jerome C, McLeod K, Bain S. Mechanical strain, induced noninvasively in the high-frequency domain, is anabolic to cancellous bone, but not cortical bone. *Bone*. 2002;**30**(3):445–452.

27. Lee NK, Sowa H, Hinoi E, Ferron M, Ahn JD, Confavreux C, Dacquin R, Mee PJ, McKee MD, Jung DY, Zhang Z, Kim JK, Mauvais-Jarvis F, Ducy P, Karsenty G. Endocrine regulation of energy metabolism by the skeleton. *Cell*. 2007;**130**(3):456–469.

28. Lee NK, Karsenty G. Reciprocal regulation of bone and energy metabolism. *Trends Endocrinol Metab*. 2008;**19**(5):161–166.

29. Ferron M, Hinoi E, Karsenty G, Ducy P. Osteocalcin differentially regulates beta cell and adipocyte gene expression and affects the development of metabolic diseases in wild-type mice. *Proc Natl Acad Sci USA*. 2008;**105**(13):5266–5270.

30. Ferron M, McKee MD, Levine RL, Ducy P, Karsenty G. Intermittent injections of osteocalcin improve glucose metabolism and prevent type 2 diabetes in mice. *Bone*. 2012;**50**(2):568–575.

31. Kindblom JM, Ohlsson C, Ljunggren O, Karlsson MK, Tivesten A, Smith U, Mellstrom, D. Plasma osteocalcin is inversely related to fat mass and plasma glucose in elderly Swedish men. *J Bone Miner Res*. 2009;**24**(5):785–791.

32. Bao Y, Ma X, Yang R, Wang F, Hao Y, Dou J, He H, Jia W. Inverse relationship between serum osteocalcin levels and visceral fat area in Chinese men. *J Clin Endocrinol Metab*. 2013;**98**(1):345–351.

33. Starup-Linde J, Eriksen SA, Lykkeboe S, Handberg A, Vestergaard P. Biochemical markers of bone turnover in diabetes patients—a meta-analysis, and a methodological study on the effects of glucose on bone markers. *Osteoporos Int*. 2014;**25**(6):1697–1708.

34. Arounleut P, Bowser M, Upadhyay S, Shi XM, Fulzele S, Johnson MH, Stranahan AM, Hill WD, Isales CM, Hamrick MW. Absence of functional leptin receptor isoforms in the POUND (Lepr(db/lb)) mouse is associated with muscle atrophy and altered myoblast proliferation and differentiation. *PLoS One*. 2013;**8**(8):e72330.

35. Erion JR, Wosiski-Kuhn M, Dey A, Hao S, Davis CL, Pollock NK, Stranahan AM. Obesity elicits interleukin 1-mediated deficits in hippocampal synaptic plasticity. *J Neurosci*. 2014;**34**(7):2618–2631.

36. Wenger KH, Freeman JD, Fulzele S, Immel DM, Powell BD, Molitor P, Chao YJ, Gao HS, Elsalanty M, Hamrick MW, Isales CM, Yu JC. Effect of whole-body vibration on bone properties in aging mice. *Bone*. 2010;**47**(4):746–755.

37. Dey A, Hao S, Erion JR, Wosiski-Kuhn M, Stranahan AM. Glucocorticoid sensitization of microglia in a genetic mouse model of obesity and diabetes. *J Neuroimmunol*. 2014;**269**(1-2):20–27.

38. Scheufele F, Wolf B, Kruse M, Hartmann T, Lempart J, Muehlich S, Pfeiffer AF, Field LJ, Charron MJ, Pan ZQ, Engelhardt S, Sarikas A. Evidence for a regulatory role of Cullin-RING E3 ubiquitin ligase 7 in insulin signaling. *Cell Signal*. 2014;**26**(2):233–239.

39. Stranahan AM, Lee K, Martin B, Maudsley S, Golden E, Cutler RG, Mattson MP. Voluntary exercise and caloric restriction enhance hippocampal dendritic spine density and BDNF levels in diabetic mice. *Hippocampus*. 2009;**19**(10):951–961.

40. Stranahan AM, Cutler RG, Button C, Telljohann R, Mattson MP. Diet-induced elevations in serum cholesterol are associated with alterations in hippocampal lipid metabolism and increased oxidative stress. *J Neurochem*. 2011;**118**(4):611–615.

41. Folch J, Lees M, Sloane Stanley GH. A simple method for the isolation and purification of total lipides from animal tissues. *J Biol Chem*. 1957;**226**(1):497–509.

42. Herberg S, Kondrikova G, Hussein KA, Periyasamy-Thandavan S, Johnson MH, Elsalanty ME, Shi X, Hamrick MW, Isales CM, Hill WD. Total body irradiation is permissive for mesenchymal stem cell-mediated new bone formation following local transplantation. *Tissue Eng Part A*. 2014;**20**(23-24):3212–3227.

43. McGee-Lawrence ME, Stoll DM, Mantila ER, Fahrner BK, Carey HV, Donahue SW. Thirteen-lined ground squirrels (Ictidomys tridecemlineatus) show microstructural bone loss during hibernation but preserve bone macrostructural geometry and strength. *J Exp Biol*. 2011;**214**(8):1240–1247.

44. Jing D, Luo E, Cai J, Tong S, Zhai M, Shen G, Wang X, Luo Z. Mechanical vibration mitigates the decrease of bone quantity and bone quality of leptin receptor-deficient db/db mice by promoting bone formation and inhibiting bone resorption. *J Bone Miner Res*. 2016;**31**(9):1713–1724.

45. Liu Y, Zhai M, Guo F, Shi T, Liu J, Wang X, Zhang X, Jing D, Hai C. Whole body vibration improves insulin resistance in db/db mice: amelioration of lipid accumulation and oxidative stress. *Appl Biochem Biotechnol*. 2016;**179**(5):819–829.

46. Rubin CT, Capilla E, Luu YK, Busa B, Crawford H, Nolan DJ, Mittal V, Rosen CJ, Pessin JE, Judex S. Adipogenesis is inhibited by brief, daily exposure to high-frequency, extremely low-magnitude mechanical signals. *Proc Natl Acad Sci USA*. 2007;**104**(45):17879–17884.

47. Luu YK, Ozcivici E, Capilla E, Adler B, Chan E, Shroyer K, Rubin J, Judex S, Pessin JE, Rubin CT. Development of diet-induced fatty liver disease in the aging mouse is suppressed by brief daily exposure to low-magnitude mechanical signals. *Int J Obes*. 2010;**34**(2):401–405.

48. Maddalozzo GF, Iwaniec UT, Turner RT, Rosen CJ, Widrick JJ. Whole-body vibration slows the acquisition of fat in mature female rats. *Int J Obes*. 2008;**32**(9):1348–1354.

49. Huang CC, Tseng TL, Huang WC, Chung YH, Chuang HL, Wu JH. Whole-body vibration training effect on physical performance and obesity in mice. *Int J Med Sci*. 2014;**11**(12):1218–1227.

50. Yokoyama C, Wang X, Briggs MR, Admon A, Wu J, Hua X, Goldstein JL, Brown MS. SREBP-1, a basic-helix-loop-helix-leucine zipper protein that controls transcription of the low density lipo-protein receptor gene. *Cell.* 1993;**75**(1):187–197.

51. Lin CI, Huang WC, Chen WC, Kan NW, Wei L, Chiu YS, Huang CC. Effect of whole-body vibration training on body composition, exercise performance and biochemical responses in middle-aged mice. *Metabolism.* 2015;**64**(9):1146–1156.

52. Khan MP, Singh AK, Joharapurkar AA, Yadav M, Shree S, Kumar H, Gurjar A, Mishra JS, Tiwari MC, Nagar GK, Kumar S, Ramachandran R, Sharan A, Jain MR, Trivedi AK, Maurya R, Godbole MM, Gayen JR, Sanyal S, Chattopadhyay N. Patho-physiological mechanism of bone loss in type 2 diabetes involves inverse regulation of osteoblast function by PGC-1α and skeletal muscle atrogenes: AdipoR1 as a potential target for reversing diabetes-induced osteopenia. *Diabetes.* 2015;**64**(7):2609–2623.

53. Ceccarelli G, Benedetti L, Galli D, Prè D, Silvani G, Crosetto N, Magenes G, Cusella De Angelis MG. Low-amplitude high fre-quency vibration down-regulates myostatin and atrogin-1 ex-pression, two components of the atrophy pathway in muscle cells. *J Tissue Eng Regen Med.* 2014;**8**(5):396–406.

54. Warmington SA, Tolan R, McBennett S. Functional and histo-logical characteristics of skeletal muscle and the effects of leptin in the genetically obese (ob/ob) mouse. *Int J Obes Relat Metab Disord.* 2000;**24**(8):1040–1050.

55. McPherron AC, Lee S-J. Suppression of body fat accumulation in myostatin-deficient mice. *J Clin Invest.* 2002;**109**(5):595–601.

56. Qiu S, Mintz JD, Salet CD, Han W, Giannis A, Chen F, Yu Y, Su Y, Fulton DJ, Stepp DW. Increasing muscle mass improves vascular function in obese (db/db) mice. *J Am Heart Assoc.* 2014;**3**(3): e000854.

57. Pedersen BK, Febbraio MA. Muscles, exercise and obesity: skeletal muscle as a secretory organ. *Nat Rev Endocrinol.* 2012;**8**(8):457–465.

58. Gundberg CM, Lian JB, Booth SL. Vitamin K-dependent carboxyl-ation of osteocalcin: friend or foe? *Adv Nutr.* 2012;**3**(2):149–157.

59. Booth SL, Centi A, Smith SR, Gundberg C. The role of osteocalcin in human glucose metabolism: marker or mediator? *Nat Rev Endocrinol.* 2013;**9**(1):43–55.

60. Du J, Zhang M, Lu J, Zhang X, Xiong Q, Xu Y, Bao Y, Jia W. Osteocalcin improves nonalcoholic fatty liver disease in mice through activation of Nrf2 and inhibition of JNK. *Endocrine.* 2016;**53**(3):701–709.

61. Shen H, Grimston S, Civitelli R, Thomopoulos S. Deletion of connexin43 in osteoblasts/osteocytes leads to impaired muscle formation in mice. *J Bone Miner Res.* 2015;**30**(4):596–605.

62. Yoshikawa Y, Kode A, Xu L, Mosialou I, Silva BC, Ferron M, Clemens TL, Economides AN, Kousteni S. Genetic evidence points to an osteocalcin-independent influence of osteoblasts on energy metabolism. *J Bone Miner Res.* 2011;**26**(9):2012–2025.

63. Sañudo B, Alfonso-Rosa R, Del Pozo-Cruz B, Del Pozo-Cruz J, Galiano D, Figueroa A. Whole body vibration training improves leg blood flow and adiposity in patients with type 2 diabetes mellitus. *Eur J Appl Physiol.* 2013;**113**(9):2245–2252.

64. Franz MJ, Boucher JL, Rutten-Ramos S, VanWormer JJ. Lifestyle weight-loss intervention outcomes in overweight and obese adults with type 2 diabetes: a systematic review and meta-analysis of randomized clinical trials. *J Acad Nutr Diet.* 2015;**115**(9): 1447–1463.

65. Delahanty LM, Dalton KM, Porneala B, Chang Y, Goldman VM, Levy D, Nathan DM, Wexler DJ. Improving diabetes outcomes through lifestyle change–A randomized controlled trial. *Obesity (Silver Spring).* 2015;**23**(9):1792–1799.